SAR Imaging of Moving Targets using Polynomial FT

Igor Djurović, Thayananthan Thayaparan, LJubiša Stanković

Abstract— **The polynomial Fourier transform is employed as a tool for the SAR imaging of moving targets. An efficient algorithm is proposed that can be used for radar images containing both moving and stationary targets. The proposed algorithm can be used in a form of the second order polynomial FT, but it can also be extended to higher order and order adaptive polynomial FT forms.**

I. Introduction

SAR imaging in the case of both moving and non-moving components within the same radar image is a challenging problem. Non-moving targets are well focused in the Fourier domain after compensation of the second-order term in the signal phase caused by the radar (platform) motion. However, radar images of moving targets could be spread (defocused) and dislocated from the true positions [1]. At the same time, focusing of moving targets in the radar image implies defocusing of non-moving targets. Several techniques are employed in the open literature to treat the problem of defocusing both moving and non-moving targets in SAR images.

Different tools are used for SAR imaging in this case:

- Phase differentiation techniques are the simplest in the field and very accurate for monocomponent signals [2]. The discrete polynomial transforms belong to this group of techniques [2]-[4]. However, they cannot be accurately used for multicomponent signals due to interferences between signal components;

- Polynomial higher order ambiguity functions (PHAF) remove cross-terms but they could introduce spurious components. In addition they can have problems with unknown number of signals and/or model of phase of the signal of interest [5];

- Integrated generalized ambiguity functions (IGAF) remove the cross-terms but they are very demanding due to the employed 2D search. Also, this technique could suffer from the unknown order of polynomial in signal phase [6];

- Improvement in the time-frequency or joint space/spatial frequency domain by using time-frequency representations [7]. This could be very useful for numerous radar images. However, due to the smoothing of cross-terms the desired signal components would also be smoothed. Then, it would be very difficult to distinguish close reflectors.

In this paper, we will consider a technique that can be used for radar signals where a single return contains information on several targets, some of them are moving (with different parameters) and some are non-moving. First, we will perform the standard radar imaging [8] based on the Fourier transform (FT) of the received signal. Then, all the components that are well-focused in the FT domain will be separated from the non-focused ones. For non-focused components in the FT domain we apply the polynomial FT (PFT) of the second order. Focused components from this domain are removed and the procedure is repeated until all signal components are recognized. Eventually, if we detect that the radar return contains signal component of significant energy that it is not focused yet with the PFT of the second order, we can proceed with the PFT of higher order. Similar technique is proposed in [9]. It is called the order-adaptive PFT. The proposed technique is based on linear transform with respect to the signal. It can produce the same or similar resolution in radar imaging as the resolution of the FT based techniques but with improved concentration of components. However, due to the motion caused effect, the problem of dislocating the radar tar-

gets from proper positions remains. This effect is studied in details in [10] with several approaches for its reduction.

The manuscript is organized as follows. After review of the radar signal model in Section II and PFT in Section III, an algorithm for focusing radar images containing both moving and stationary targets is described in Section IV. Numerical examples are given in Section V. Concluding remarks and possible extension of the approach are discussed in Section VI.

II. Model of radar system

In order to describe the SAR imaging problem for images containing both moving and stationary targets, we will consider a well known model of SAR system from [1]. This model is presented in Fig. 1.

Assume that the signal transmitted toward radar target is of the form: $s_T(t) = \exp\{j2\pi(f_0 t + \eta t^2/2)\}$, $0 \le t \le T$, where f_0 is the carrier frequency, while η is referred to as a chirp-rate. The received signal is attenuated and delayed with respect to the transmitted signal. The baseband version of the received signal after range compensation can be written as:

$$s_R(t) = C_0 \exp\left\{-j\frac{4\pi R(t)}{\lambda}\right\} \times \text{sinc}\left[\pi\eta\delta T\left(t - 2R(t)/c\right)\right], \quad (1)$$

where C_0 is a constant corresponding to the reflectivity coefficient of the radar target, λ is wavelength, δT is the width of compressed pulse, and c is velocity of light. For a moving target the distance between the radar and the target can be written as eq. 2 (at the top of the next page.)

Note that v is the aircraft velocity, (v_x, v_y) and (a_x, a_y) are the target velocity and acceleration in corresponding directions, h is the altitude of the platform (aircraft) while (x_0, y_0) is the target position with radar mounted on the board of the aircraft. The Taylor series expansion of $R(t)$ produces:

$$R(t) \simeq R(0) + R'(0)t + R''(0)t^2/2 = R_0 + \frac{x_0 v_x + y_0 v_y - x_0 v}{R_0}t + \frac{v^2 + v_x^2 + v_y^2 + x_0 a_x + y_0 a_y - 2v v_x}{2R_0}t^2, \quad (3)$$

where $R_0 = \sqrt{x_0^2 + y_0^2 + h^2}$. For non-moving target the relation $R(t) \approx R_0 - x_0 vt/R_0$ holds (with compensated term $v^2t^2/2R_0$) and the received signal (for compensated term $t = 2R(t)/c$) is:

$$s_0(t) = C_0 \exp\{-j4\pi R_0/\lambda + j4\pi x_0 vt/R_0\lambda\}. \quad (4)$$

This signal is well-concentrated in the FT domain at the frequency proportional to x_0, i.e., at $2x_0 v/R_0\lambda$.

By assuming that $x_0 \ll R_0$ and $R_0 \approx y_0$, for moving targets we have additional terms in the signal phase, producing the signal:

$$s_0(t) \approx C_0 \exp\{-j4\pi R_0/\lambda + j4\pi x_0 vt/R_0\lambda\} \times \exp\{-j2\pi 2v_y t/\lambda\} \times \exp\left\{-j4\pi[(v - v_x)^2 + v_y^2 + R_0 a_y]t^2/2R_0\lambda\right\}. \quad (5)$$

From this derivation we can conclude that the baseband return is shifted for $2v_y/\lambda$ due to the motion in the y direction. Also, the quadratic phase term, equal to $4\pi[(v - v_x)^2 + v_y^2 + R_0 a_y]t^2/2R_0\lambda$, causes spread of components. Note that we can again assume that the term caused by the aircraft motion is compensated, reducing the chirp-rate of the spreading component to approximately $4\pi[v_x^2 + v_y^2 + R_0 a_y]t^2/2R_0\lambda$.

From (5) one can conclude that there are two negative effects caused by the motion of targets: shift and defocusing introduced by higher order derivatives in the signal phase. Focusing of moving targets image by compensating the chirp-rate of (5) ($\approx 4\pi[v_x^2 + v_y^2 + R_0 a_y]/2R_0\lambda$) would cause spread in radar image of non-moving targets. It means that we have to apply different kinds of processing of signals received by various radar targets. To this aim, we apply a simple algorithm for separation of signals from the mixture and focusing each signal by using the PFT of the second order proposed for ISAR systems in [11]. However, some recent surveys and experiments have shown that for some realistic applications, including traffic monitoring, the received signal has polynomial phase of order

$$R(t) = \sqrt{(vt - v_x t - a_x t^2/2 - x_0)^2 + (y_0 + v_y t + a_y t^2/2)^2 + h^2}. \quad (2)$$

higher than 2. For details on these experiments refer to [7], [12]. For this case our approach can easily be upgraded employing the order adaptive PFT [9].

Note that the backprojection technique is considered recently for the SAR imaging as an alternative to the considered radar model. This technique stems from the computer tomography [13], [14]. There are several advantages of this technique including using of the polar instead of the Cartesian coordinate system. In this case, the polar system more accurately describes considered problem. In addition, processing of radar images in the case of the backprojection algorithm can be performed pixel-by-pixel (employing some interpolation strategy) without waiting for all radar returns. The backprojection algorithm has relatively high computational complexity that requires some sort of parallel processing in order to achieve real time calculation. However, radar model in this paper assumes that radar target is relatively far from the aircraft platform as in [7]. It means that errors caused by using the Cartesian are small comparing to the polar coordinate system. Thus we will continue to study problem of SAR imaging with the FT based approach.

III. Polynomial FT

Here, we will describe the PFT that will be used as a tool for SAR images focusing. As far as we know the PFT of the second order is used in [15] for detecting moving targets but not for imaging. Our approach has several advantages with respect to this technique since we can efficiently calculate the PFT of the higher order polynomial phase signals (PPS) using order adaptive PFT form [9]. In addition, since the chirp-rate that corresponds to the moving object is relatively slowly varying our approach offers possibility to perform search for chirp parameters over reduced parameter space. Note that the PFT is applied in the ISAR imagining in [11]. However, the algorithm in the case of SAR images is significantly different due to different type of targets and radar parameters.

The standard FT of discrete-time signals can be defined as:

$$X(\omega) = \sum_n x(n) \exp(-j\omega n) \quad (6)$$

where it is assumed that the signal $x(n)$ is a discretized version of the continuous time signal $x(n) = x(n\Delta t)$, sampled with sampling rate Δt selected according to the sampling theorem. For sinusoidal signal $x(t) = \exp(j\omega_0 t)$, the FT is concentrated on the frequency $\omega = \omega_0$, i.e., $X(\omega) = 2\pi\delta(\omega - \omega_0)$ for signal with relatively large number of samples. Then, we can perform the estimation of the frequency of sinusoid by using the FT as:

$$\hat{\omega}_0 = \arg\max_{\omega} |X(\omega)|. \quad (7)$$

However, for the PPS $x(n) = \exp(j\phi(n))$, with $\phi(n) = \sum_{k=1}^{\infty} a_k n^k$ the FT exhibits:

$$X(\omega) \approx 2\pi\delta(\omega - \phi'(0)) *_\omega FT\left\{\exp\left(j\sum_{k=2}^{\infty}\phi^{(k)}(0)n^k/k!\right)\right\}, \quad (8)$$

where $\phi'(0)$ and $\phi^{(k)}(0)$, $k = 2, 3, ...$ represent respectively the first and higher-order derivatives of the signal phase evaluated for $n = 0$ (i.e., for $t = 0$), and $*_\omega$ denotes the frequency domain convolution. Obviously, the problem of signal parameters estimation from (8) is not trivial. We need more sophisticated tools than the simple FT. In addition, $X(\omega)$ given in (8) is spread in the frequency domain due to the term $FT\left\{\exp\left(j\sum_{k=2}^{\infty}\phi^{(k)}(0)n^k/k!\right)\right\}$ caused by the higher order derivatives. One of the ideas is to perform the phase differentiation by using the correlation of signal in the time domain [2], [6]. They have proposed decreasing the order of polynomial in the signal phase until a sinusoidal signal is obtained. By using the FT of this signal we can determine

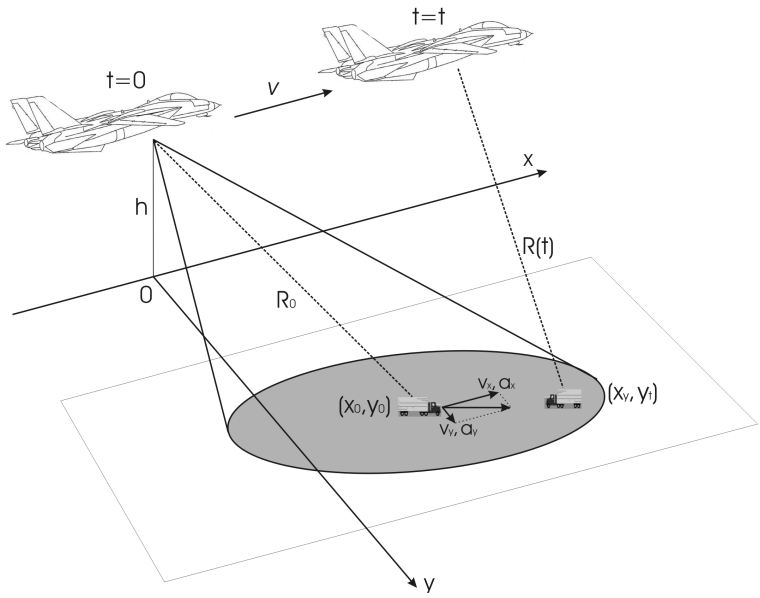

Fig. 1. Model of SAR system.

the coefficient of the highest polynomial in the signal phase. The estimated coefficient of the highest order term in polynomial expansion is used in the estimation of the lower order coefficients. This procedure is not accurate in the case of multicomponent signals since autocorrelations would have cross-terms caused by multiple components. In addition, errors in estimation of the highest order coefficients propagate to estimation of lower order coefficients.

The PFT is reinvented several times in science under different names [16]-[18]. Detailed asymptotic accuracy analysis of this transform is performed in [19], [20]. The PFT can be defined as:

$$X(\omega;\alpha_2,\alpha_3,...,\alpha_k) = \sum_n x(n)\exp(-j\omega n - j\alpha_2 n^2 - j\alpha_3 n^3 - ... - j\alpha_k n^k). \quad (9)$$

Obviously, for the PPS of the $k-$th order, $x(n) = \exp\left(j\sum_{l=1}^{k} a_l n^l\right)$, the PFT will be ideally concentrated at the position corresponding to the signal parameters $\omega = a_1$, $\alpha_l = a_l$ for $l = 2, ..., k$. Then, parameters of the PPS of the $k-$th order can be estimated by using position of the PFT maximum:

$$(\hat{a}_1, \hat{a}_2, ..., \hat{a}_k) = \arg \max_{(\omega,\alpha_2,...,\alpha_k)} |X(\omega;\alpha_2,\alpha_3,...,\alpha_k)|. \quad (10)$$

The PFT for signals of the corresponding order (when the order of polynomial in signal phase is the same as the order of the PFT) is the maximum likelihood (ML) estimate of the PPS parameters. However, the remaining problem is in dimensionality that can introduce significant memory and calculation requirements. An additional problem could be mismodeling (using the higher order PFT to capture signals with lower order of polynomial in the phase or using the lower order PFT to capture higher order of polynomial in the signal phase). However, our goal is to obtain a focused SAR image but not to perform extremely precise signal parameters estimation. It is more important that radar images are focused, as high as possible, and that the calculation requirement is within reasonable limits. Both of these effects can be achieved by using

the PFT of the second order:

$$X(\omega;\alpha)=\sum_n x(n)\exp(-j\omega n-j\alpha n^2). \quad (11)$$

For signal $x(n)=\exp(j\omega_0 n+jan^2)$ the ideal concentration on central frequency $\omega=\omega_0$ can be achieved for $\alpha=a$. Thus, our goal is to estimate the parameter a, $\alpha=\hat{a}$ in order to concentrate (focus) the signal (radar image) on the frequency $\omega=\omega_0$ (position). When the signal contains higher order polynomial in the signal phase, we have two possible strategies. The first is to assume that higher order derivatives (third and other higher order) do not contribute significantly to spreading components and to perform the procedure as in the case of the signals of the second order polynomial in the phase. The second strategy is to employ the recently proposed order adaptive PFT approach [9] where in each stage of the procedure the order of polynomial in the signal phase is increased until the well concentrated signal component is obtained. Then, instead of multidimensional search for signal parameters over $k-$dimensional parameter space, the procedure is reduced to k searches over an $1-$dimensional parameter space.

The main advantages of the approach based on the PFT are its closeness to the ML estimate (it means that this technique is robust to noise influence) and at the same time this transform is linear (there are no effects associated to the cross-terms). In the next section, a procedure for focusing SAR image based on the PFT is introduced.

IV. Algorithm for Imaging of Moving Targets

Signals received from radar target will be denoted as: $s_0(t,m)$, $m=0,...,M-1$, where m represents the chirp index. We assume that the signal is sampled with sampling rate $\Delta t=T/N$, $s_0(n,m)=s_0(n\Delta t,m)$. The standard radar image can be obtained as a 2D FT of the dechirped version of received signal:

$$S(\omega_n,\omega_m)=FT\{s_0(n,m)\}=$$

$$\sum_n\sum_m s_0(n,m)\exp(-j\omega_n n-j\omega_m m). \quad (12)$$

This radar image can be alternatively represented by using two 1D FTs as:

$$S(\omega_n,\omega_m)=\sum_m S_0(\omega_n,m)\exp(-j\omega_m m), \quad (13)$$

where

$$S_0(\omega_n,m)=\sum_n s_0(n,m)\exp(-j\omega_n n). \quad (14)$$

The obtained image could be non-focused for the moving targets, as well as dislocated from the proper position. Now we will describe the algorithm for focusing the radar target.

Algorithm

FOR each m

Let $\rho(n,m)=s_0(n,m)$ and $R(\omega_n,m)=\sum_n\rho(n,m)\exp(-j\omega_n n)$ and $I=1$, $\hat{\alpha}_I=0$.

WHILE radar return $\rho(n,m)$ contains significant energy

Calculate

$$S_I(\omega_n,m)=R(\omega_n,m) \quad (15)$$

for (ω_n,m) representing well-focused component (target) in the FT domain and $S_I(\omega_n,m)=0$ otherwise. Non-focused components are updated as: $R(\omega_n,m)\leftarrow R(\omega_n,m)-S_I(\omega_n,m)$. Calculate

$$\rho(n,m)=IFT\{R(\omega_n,m)\exp(j\hat{\alpha}_I n^2)\}. \quad (16)$$

Set $I\leftarrow I+1$.

FOR $\alpha\in\Lambda$ (for various chirp-rates from the considered set Λ)

Calculate

$$R_\alpha(\omega_n,m)=\sum_n\rho(n,m)\exp(-j\omega_n n-j\alpha n^2). \quad (17)$$

ENDFOR

Estimate the chirp-rate of the radar returns as:

$$(\hat{\alpha}_I,\hat{\omega}_{n_I})=\arg\max_{(\alpha,\omega_n)}|R_\alpha(\omega_n,m)|,$$

$$R(\omega_n,m)=R_{\hat{\alpha}_I}(\omega_n,m). \quad (18)$$

ENDWHILE

ENDFOR

Radar image is calculated as:

$$S(\omega_n,\omega_m)=$$

$$= \sum_{J=1}^{I} \sum_{m} S_J(\omega_n, m) \exp(-j\omega_m m). \tag{19}$$

Comments to the algorithm.

1. There are several ideas how to determine what is relatively high energy. For noiseless signal it can be determined by using the following technique. If the total energy is $\sum_n \sum_m |s_0(n,m)|^2$, then the average energy in a single return is $\sum_n \sum_m |s_0(n,m)|^2/M$. We are considering only chirps (or chirps with already removed components) $\rho(n,m)$ with energy larger than $\varepsilon \sum_n \sum_m |s_0(n,m)|^2/M$, where ε is a small positive number. In simulations, the conservative value of $\varepsilon = 0.02$ is adopted producing significant calculation savings for noiseless signals.

However, in the case of signals corrupted by certain amount of noise, this technique does not produce any savings of calculations and we need some alternative way for reducing the number of received chirps for which the search is performed. For this purpose the noise variance is estimated. Here, we will describe the procedure for the Gaussian additive noise environment, while similar techniques could be developed for other noise environments and models of clutter and backscatter data [21]. Under the assumption that the noise environment is Gaussian, the variance can be estimated as [22], [23]:

$$\hat{\sigma}^2 = \hat{\sigma}_R^2 + \hat{\sigma}_I^2 \tag{20}$$

$$\hat{\sigma}_R^2 = \frac{1}{M} \sum_m \hat{\sigma}_R^2(m)$$

$$\hat{\sigma}_I^2 = \frac{1}{M} \sum_m \hat{\sigma}_I^2(m) \tag{21}$$

where

$$\hat{\sigma}_R(m) = \frac{\text{median}\{|\,\text{Re}\{\rho(n+1,m) - \rho(n,m)\}|\}}{0.6745\sqrt{2}}$$

$$\hat{\sigma}_I(m) = \frac{\text{median}\{|\,\text{Im}\{\rho(n+1,m) - \rho(n,m)\}|\}}{0.6745\sqrt{2}}. \tag{22}$$

Relation (22) is a well-known estimator of the standard deviation of the Gaussian noise. In this case estimates are calculated for each m and averaged using (21). Final estimate of the variance is performed by summing estimated variances for the real and imaginary parts. Then, the threshold can be set as: $\kappa N \hat{\sigma}^2$ where N is the number of samples within single chirp and κ is a constant. We set $\kappa = 3$, i.e., a received chirp should have at least three average noise variances in order to be distinguished from the noise. Similar results can be achieved for κ in a wide range of values $\kappa \in [1, 10]$. An alternative technique for estimation of the noise variance for this type of signals is described in [24]. In addition, we can perform the estimation of the amplitude of the useful signal based on techniques described in [23] or [24] and we could set threshold based on both the estimation of the signal amplitude and the noise variance estimation. Note that the proposed variance estimation procedure could be performed for each instant n by estimating the standard deviations for fixed n as $\hat{\sigma}_R(n) = \text{median}\{|\,\text{Re}\{\rho(n,m+1) - \rho(n,m)\}|\}/0.6745\sqrt{2}$ and in similar manner for the imaginary part of noise. The obtained variance estimate should be averaged. This can produce more accurate results since signal $\rho(n,m)$ varies more slowly along the m coordinate than along the n coordinate (this estimator of the variance is proposed under stationary signal assumption). In addition, estimates $\hat{\sigma}_R(n)$ and $\hat{\sigma}_I(n)$ could be more accurate due to the reason that a significant part of the blurring occurs in the cross-range domain. However, relations (22) could be used to produce the noise variance estimate for each chirp (equal to $\kappa N[\hat{\sigma}_R^2(m) + \hat{\sigma}_I^2(m)]$) and for selecting different threshold values for each chirp what could be reasonable solution for applications when radar image is formed by using a large number of chirps and when noise parameters could be varying for various chirps.

2. The next question, arising from the proposed procedure, is how to detect well concentrated components $S_I(\omega_n, m)$. These components are higher than some specific threshold but they should also be relatively sharp local maxima. We assume that (ω_n, m) belongs to the well focused region of the radar image if:

$$|R(\omega_n, m)| > \varepsilon' \max_{\omega_n} |R(\omega_n, m)| \tag{23}$$

and:

$$|R(\omega_n, m)| > \eta_i |R(\omega_n \pm i\Delta\omega, m)|,\ i = 1, 2. \tag{24}$$

The purpose of the first condition in (23) is to remove the components with very small magnitude comparing to the maximum of $|R(\omega_n, m)|$ for a given chirp m. The second condition selects only well concentrated local maximum. For example, if the von Hann window is applied to the FT we know that the maximum of the sinusoid on the frequency grid has magnitude twice of the magnitude of the FT in neighbor samples. Then if we find this kind of pattern we can assume that we detected a highly concentrated component (well focused signal in the SAR image). In order to be more robust to the noise influence and to deal with potential application of alternative window functions, we adopted the coefficients $\eta_1 = 2$ and $\eta_2 = 4$. If $(\hat{\omega}_n, m)$, for the considered α, belongs to useful component, then we assume that samples separated by less than $2\Delta\omega$ from $\hat{\omega}_n$ belong also to the useful focused component:

$$S_I(\omega_n, m) = \\ = \begin{cases} R(\omega_n, m) & \text{for } |\omega_n - \hat{\omega}_n| \le 2\Delta\omega \\ 0 & \text{elsewhere.} \end{cases} \tag{25}$$

Note that $\Delta\omega$ is the frequency sampling distance in ω_n direction and it depends on the sampling rate $\Delta t = T/N$. This value exhibits $\Delta\omega = 2\pi/T$ but it can be translated to the position of the radar target. Namely, the resolution in x domain in the radar image is equal to $\Delta x = R_0\lambda/2vT$.

Note that $R(\omega_n, m)$ can have several highly concentrated components. These components represent targets moving with similar parameters. For example cars going over the road in the same directions. Then all targets that are highly concentrated can be removed from further analysis in this stage and we can proceed with searching for components with different chirp-rates.

3. In the case when the radar return $\rho(n, m)$ contains significant energy but we cannot detect highly concentrated component it can be assumed that this component has a form of the higher-order PPS. Then we can apply the order adaptive PFT as:

$$R_{\hat{\alpha}_I,\beta}(\omega_n, m) = \\ = \sum_n \rho(n, m) \exp(-j\omega_n n - j\hat{\alpha}_I n^2 - j\beta n^3)$$

$$(\hat{\beta}_I, \hat{\omega}_{n_I}) = \arg \max_{(\beta,\omega_n)} |R_{\hat{\alpha}_I,\beta}(\omega_n, m)|. \tag{26}$$

We can set $R(\omega_n, m) = R_{\hat{\alpha}_I,\hat{\beta}_I}(\omega_n, m)$ and remove the highly concentrated components. After removing highly concentrated components from $R(\omega_n, m)$, signal $\rho(n, m)$, that will be used for selection of other signal components, can be obtained as:

$$\rho(n, m) = IFT\{R(\omega_n, m) \exp(j\hat{\alpha}_I n^2 + j\hat{\beta}_I n^3)\}. \tag{27}$$

The procedure could be generalized to search for higher order coefficients as well. However, in our experiments it has been shown that the order three is commonly enough for radar images of our interest and that further increasing of the polynomial order could introduce problems with noise influence and with overmodeling signal phase.

4. The proposed technique does not solve the problem of displacement of the radar target from the true position caused by the motion in y direction. Techniques for reducing (removing) the displacement are studied in [10], [25]-[28]. Kirscht has proposed to consider multiple frames of radar image and to perform motion parameters estimation based on standard algorithms from video signals processing [27], [29]. Then the estimated velocity v_y can be used for the compensation of displacement in (5). The same procedure can be performed for the proposed PFT-based radar imaging. In addition, the PFT technique does not require the estimation of chirp-rates for each frame since it can be assumed that the chirp-rate varies relatively slowly. In the worst case scenario, the search for the chirp-rate in subsequent frames should be performed over very small number of chirp-rate parameters around the chirp-rate detected for previous frame. This is an important advantage of the proposed technique that helps in keeping the computational requirements within reasonable limits.

5. Performing fair comparison of calculation complexity of the proposed algorithm and standard SAR radar imaging is quite difficult. Namely, complexity of the proposed algorithm depends on the shape of the radar image, i.e., number of moving objects, number of moving objects with different motion parameters, and size of radar targets. Before we give some data about complexity of the proposed algorithm we should discuss two critical steps in the proposed algorithm. The first step is search of the optimal chirp-rate. This is quite complex procedure since it requires $RMN\log_2(MN)$ operations, where $M \times N$ are dimension of the radar image and R is number of chirp-rates in the set Λ. Fortunately, the suboptimal procedure proposed in [30] based on the LMS algorithm requires relatively small number of iterations (not exceeding 10) in order to get a suboptimal estimation of chirp-rate parameter. In addition, we are considering only those returns containing significant energy and we are removing other returns from further processing. Then this part of procedure has complexity of the order of magnitude $rpMN\log_2(MN)$ where $r \ll R$ (commonly $r \in [5, 10]$) and p is percentage of chirps with significant energy. In addition, we can further simplified the proposed algorithm since the large number of samples in $S(\omega_n, m)$ is set to be zero. Then it can be applied some of FFT algorithms that are using information about zero-samples [31], [32]. For radar-image of dimension $M\times N$ with in Q non-zero samples, calculation complexity of these algorithms is $O(MN\log_2 Q)$. Then complexity of the PFT in the first stage of the algorithm is of the order $O(prMN\log_2 pMN)$. However, in the next step well concentrated objects are removed from the PFT and we can calculate the PFT for the remaining radar image by removing from the PFT of radar image obtained in the previous step the PFT of the radar image of highly concentrated objects. These highly concentrated objects occupy very small part of image and again we can use simplified procedure for evaluation of the PFT from [31], [32]. In order to illustrate calculation complexity consider the following setup: size of radar image $M \times N = 256 \times 256$, number of iteration in the search for optimal chirp-rate $r = 10$, $p = 25\%$ of chirps with significant energy, 5 objects of 16 pixels each with different chirp-rates (motion parameters). Then, we need $MN\log_2 MN$ operations for calculation of the standard radar image. For the first step in evaluation of the PFT we need additional $rpMN\log_2 pMN$ operations. In the next stages for remaining 4 objects we need $4rMN\log_2 16$ operations. In total we need: 13828096 operations. The standard radar imaging requires 1048576 operations. The proposed algorithm requires about 13 times more operations for this setup than in the standard SAR imaging but this complexity has been paid off with significant improvement in the radar image quality.

V. Numerical study

The experiment is inspired by the Environment Canada's airborne CV 580 SAR system described in [7]. A high resolution radar operating at the frequency $f_0 = 5.3$GHz (frequency of the C-band of the CV 580 SAR system). The bandwidth of linear FM chirps is $B = 25$MHz, duration of the pulse is $T = 1/300$s. Signal is sampled with $\Delta t = T/N$, where $N = 256$ and number of pulses within one revisit is $M = 256$. The platform (aircraft) velocity is 130m/s. The radar altitude is $h = 6$km. For considered model the maximal difference for single cell between polar and Cartesian coordinates is about 6% (less than 40cm). In this experiment we consider the radar image containing 8 targets. Radar returns from all 8 point scatterers can be obtained by using the superposition principle, as a sum of the individual returns. In the case of stationary targets, the radar image is shown in Fig. 2a. This radar image is obtained by the 2D FT processing. It can be noticed that all targets are well concentrated (focused). However, when the targets in the corners are moving the radar image obtained with standard techniques is spread, Fig. 2b. Velocity of moving targets is represented by linear law as: $v_x^{(i)}(t) = v_x^{(i)}(0) + a_x^{(i)}t$, $v_y^{(i)}(t) = v_y^{(i)}(0) + a_y^{(i)}t$, $i = 1, 2, 3, 4$. Parameters of the motion are selected as: $\mathbf{V}_x = [v_x^{(1)}(0)\ v_x^{(2)}(0)\ v_x^{(3)}(0)\ v_x^{(4)}(0)] = [12\ -20\ 0\ -10]$m/s, $\mathbf{V}_y = [v_y^{(1)}(0)$

... $v_y^{(4)}(0)] = [0\ 10\ 20\ -20]$m/s, $\mathbf{A}_x = [a_x^{(1)}\ a_x^{(2)}\ a_x^{(3)}\ a_x^{(4)}] = [0\ 0\ 0\ 2]$m/s^2 and $\mathbf{A}_y = [0\ 0\ 1\ 0]$m/s^2. It can be seen that corner targets are dislocated and spread from the true positions. The proposed algorithm is applied with the set of chirp-rate parameters selected as $\alpha \in \Lambda = [-0.005, 0.005]$. Domain of chirp-rates can be determined according to a priory knowledge about expected maximal velocity and acceleration of the target and distance R_0. Since calculation is performed for discrete time signals, this maximal chirp-rate should be normalized by a square of the sampling rate $\Delta t = T/N$. Obtained results are presented in Fig. 2c. It can be seen that all radar targets are well focused. In order to demonstrate an advantage of our algorithm over the time-frequency representations, we are considering the signal independent S-method based radar imaging [33] that has shown good accuracy and high concentration in numerous considered trials, Fig. 2d. However, this transform cannot separate very close components in the radar image. It can be seen from Fig. 2d that on two positions, for close scatterers, we have cross-terms caused by mutual influence of signal components. These positions are marked with ellipses on Fig. 2d.

Fig. 3 depicts the same setup but now with additive Gaussian noise. All targets have the same reflectivity coefficient $C_0 = 1$. The signal is embedded in the Gaussian white additive noise with variance $\sigma^2 = 100$. It can be seen that the proposed transform works very accurately. The proposed thresholds in this case keep low number of chirps for which the proposed optimization procedure is performed. As an additional benefit, this algorithm setup rejects significant portion of the additive noise.

The third setup we consider here is common for the Ground Motion Target Identification systems (SAR/GMTI). In this setup we have 16 targets of which 8 are moving in the same direction with similar motion parameters, while other 8 targets are moving in opposite direction with similar motion parameters. These targets could illustrate moving of cars in two different directions along the same road or motion of tanks on a battlefield. In the first stage of the algorithm we recognize dominant chirp-rate corresponding to one group of targets. Then all radar images of radar targets moving in the same direction are highly concentrated (focused) and we can remove all these targets from radar image. In the next step we detect the chirp-rate parameter corresponding to other targets. Then, this procedure calculate the PFT-based image within two basic steps even if we have 16 different targets in the radar image. In Fig.4 the following radar images are given: radar image of non-moving targets (Fig. 4a), the FT-based radar image (Fig. 4b), the PFT-based radar image (Fig. 4c) and the S-method-based radar image (Fig. 4d). Again we can observe the same effect as in the previous two cases. Namely, the standard radar image of moving targets is very spread while in the case of the S-method we have cross-terms between some of radar targets. The proposed technique (PFT) produces quite good results in this case with highly concentrated targets and without interference terms.

VI. Conclusion

The PFT-based algorithm for focusing SAR images has been proposed. The algorithm can be performed in two modes: with second order PFT or with the order-adaptive PFT. The algorithm performs accurately even in relatively high noise environment. It is based on the linear signal representation and it can produce very high resolution of the radar image with moving targets that is close to the resolution of the FT for radar image with non-moving targets. The algorithm with order adaptive form of the PFT can compensate higher order polynomial in the signal phase without employing consuming search over a $k-$dimensional parameter space.

Further research will be concentrated to reduce the motion displacement effects. Also, it has recently been shown in [34] that for multi-component signals phase differentiation techniques produce suboptimal results even in the case when cross-terms are removed. Then, it would be very interesting to apply the phase differentiation (higher order ambiguity function) with non-linear optimization approach proposed in [34] in order to achieve two goals:

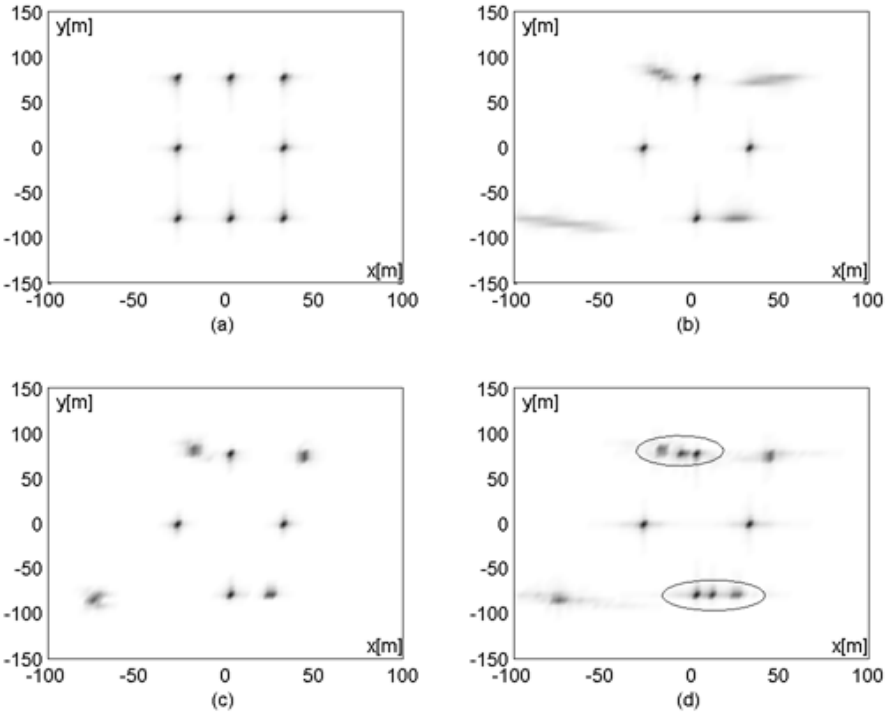

Fig. 2. SAR imaging of 8 targets: (a) Non-moving targets, FT based imaging; (b) Moving target, FT based imaging; (c) Moving target, imaging based on the proposed approach; (d) Moving target, imaging based on the SM.

focused radar image for multicomponent signals with reduced calculation complexity. In addition, the proposed approach can be applied to the newly proposed SAR systems with generalized inverse synthetic aperture radar geometry [35].

References

[1] V. C. Chen, and H. Ling, *Time-frequency transforms for radar imaging and signal analysis*, Artech House, 2003.

[2] S. Peleg, and B. Porat, "Linear FM parameter estimation from discrete time observations," *IEEE Trans. Aerosp. Electron. Syst.*, Vol. 27, No.4, July 1991, pp. 607-616.

[3] S. Golden and B. Friedlander, "A modification of the discrete polynomial transform," *IEEE Trans. Sig. Proc.*, Vol. 46, No. 5, May 1998, pp. 1452-1455.

[4] M. F. Aburdene, C. Jin, and R. J. Kozick, "Efficient computation of discrete polynomial transforms," *IEEE Sig. Proc. Let.*, Vol. 10, No. 10, Oct. 2003, pp. 285-288.

[5] S. Barbarossa, A. Scaglione and G. B. Giannakis, "Product high-order ambiguity function for multicomponent polynomial-phase signal modeling," *IEEE Trans. Sig. Proc.*, Vol. 46, No.3, Mar. 1998, pp. 691-708.

[6] S. Barbarossa and V. Petrone, "Analysis of polynomial-phase signals by the integrated generalized ambiguity function," *IEEE Trans. Sig. Proc.*, Vol. 45, No. 2, Feb. 1997, pp. 316-327.

[7] J. J. Sharma, C. H. Gierull, and M. J. Collins, "Compensating the effects of target acceleration in dual-channel SAR-GMTI," *IEE Proc. of Radar, Sonar and Navigation*, Vol. 153, No. 1, Feb. 2006, pp. 53-62.

[8] W. G. Carrara, R. S. Goodman, and R. M. Majewski, *Spotlight synthetic aperture radar - signal processing algorithms*, Artech House, 1995.

[9] LJ. Stanković, and S. Djukanović, "Order adaptive local polynomial FT based interference rejection in spread spectrum communication systems," *IEEE Trans. on Inst. and Meas.*, Vol. 54, No. 6, Dec. 2005, pp. 2156- 2162.

[10] R. K. Raney, "Synthetic aperture imaging radar and moving targets," *IEEE Trans. Aer. El. Sys.*, Vol. 7, No. 3, pp. 499-505, May 1971.

[11] I. Djurović, T. Thayaparan, and LJ. Stanković, "Adaptive Local Polynomial Fourier Transform in

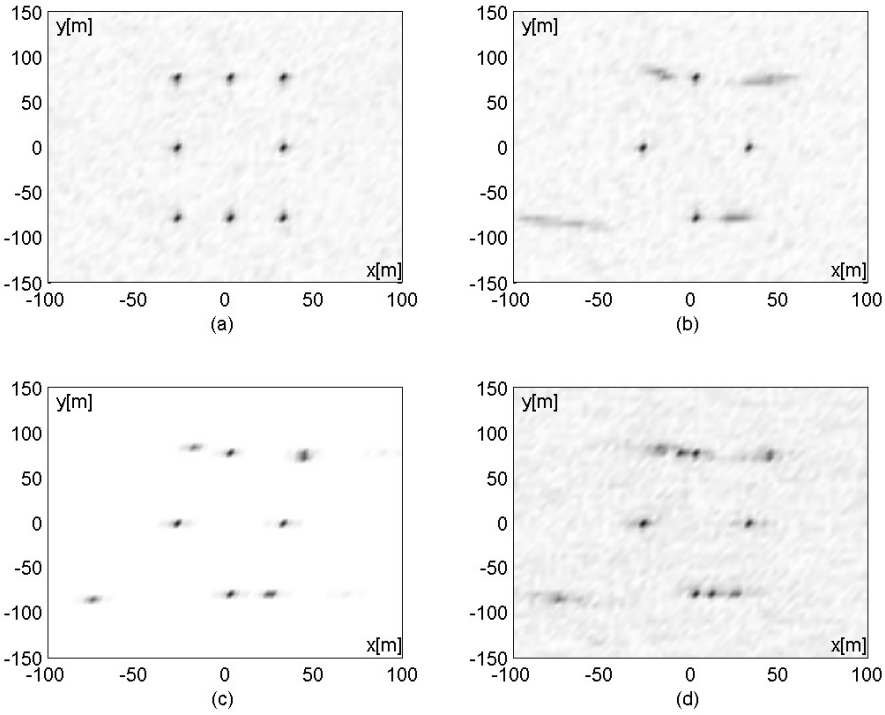

Fig. 3. SAR imaging of 8 targets for signal corrupted by white additive Gaussian noise: (a) Non-moving targets, FT based imaging; (b) Moving target, FT based imaging; (c) Moving target, imaging based on the proposed approach; (d) Moving target, imaging based on the SM.

ISAR," *Journal of Applied Signal Processing*, Article ID 36093, 2006.

[12] J. J. Sharma, C. H. Gierull, and M. J. Collins, "The Influence of target acceleration on velocity estimation in dual-channel SAR-GMTI," *IEEE Trans. Geosci. Remote Sensing*, Vol. 44, No. 1, pp. 134–135, Jan. 2005.

[13] M. D. Desai, and W. K. Jenkins, "Convolution backprojection image reconstruction for spotlight mode synthetic aperture radar," *IEEE Trans. on Im. Proc.*, Vol. 1, No. 4, Oct. 1992, pp. 505-517.

[14] L. Rosenberg, and D. Gray, "Multichannel SAR imaging with backprojection," in *Proc. of ISSNIP 2004*, pp. 265-270.

[15] C. Qu, Y. He, F. Su, and Y. Huang, "SAR moving targets detection based on the chirp-Fourier transform," in *Proc. of IEEE Radar Conf.*, May 2005, pp. 802 - 805.

[16] X.-G Xia, "Discrete chirp-Fourier transform and its application to chirp rate estimation," *IEEE Trans. on Sig. Proc.*, Vol. 48, No. 11, Nov. 2000, pp. 3122-3133.

[17] S. Mann, and S. Haykin, "The chirplet transform: physical considerations," *IEEE Trans. Sig. Proc.*, Vol. 43, No. 11, Nov. 1995, pp. 2745-2761.

[18] L. B. Almeida, "The fractional Fourier transform and time-frequency representations," *IEEE Trans. Sig. Proc.*, Vol. 42, No. 11, Nov. 1994, pp. 3084–3091.

[19] V. Katkovnik, "A new form of the Fourier transform for time-frequency estimation," *Sig. Proc.*, Vol. 47, No. 2, pp. 187-200, 1995.

[20] V. Katkovnik, "Local polynomial periodogram for time-varying frequency estimation," *South Afr. Stat. Jour.*, Vol. 29, No. 2, pp. 16, 168-195.

[21] G. Kulemin, *Millimeter-wave radar targets and clutter*, Artech House, 2003.

[22] D. L. Donoho, and I. M. Johnstone "Adapting to unknown smoothness via wavelet shrinkage," *JASA*, vol 90, 432, pp. 1200-1224, 1995.

[23] V. Katkovnik, and LJ. Stanković, "Instantaneous frequency estimation using the Wigner distribution with varying and data driven window length", *IEEE Trans. on Signal Processing*, Vol. 46, No. 9, Sept. 1998, pp. 2315-2325.

[24] S. Chandra Sekhar, and T. V. Sreenivas: "Signal-to-noise ratio estimation using higher-order moments," *Sig. Proc.*, Vol. 86, 2006, pp. 716-732.

[25] S. Barbarossa, "Detection and imaging of moving objects with synthetic aperture radar Part 1: Optimal detection and parameter estimation theory," *IEE Proc.-F*, Vol. 139, No. 1, pp. 79-88,

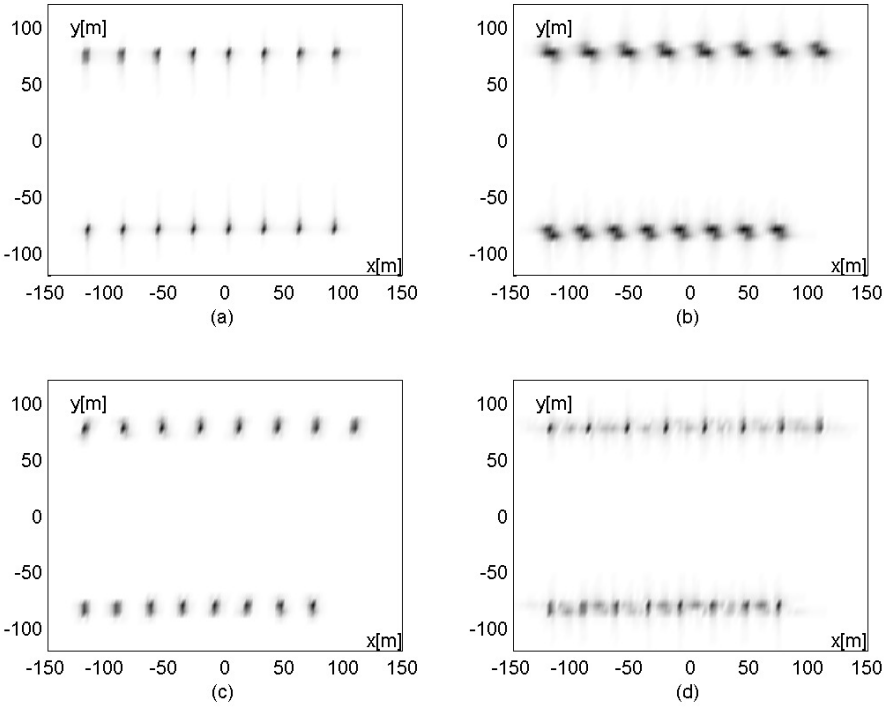

Fig. 4. SAR imaging of 16 targets: (a) Non-moving targets, FT based imaging; (b) Moving target, FT based imaging; (c) Moving target, imaging based on the proposed approach; (d) Moving target, imaging based on the SM.

1992,.

[26] S. Barbarossa, and A. Farina, "A novel procedure for detecting and focusing moving objects with SAR based on the Wigner-Ville distribution," in *Proc. of IEEE Int. Radar Conf.*, Arlington, 1990.

[27] M. Kirscht, "Detection and focused imaging of moving objects evaluating a sequence of single-look SAR images," in *Proc. of IARSC*, vol. I, pp. 393-400, July 1997.

[28] M. Bierling, "Displacement estimation by hierarchical blockmatching," in *Proc. of SPIE on Vis. Com. and Im. Proc.*, pp. 942-951, 1988.

[29] B. Barnett, "Basic concepts and techniques of video coding and the H.261 standard," in *Handbook of image & video processing*, ed. A. Bovik, pp. 777-798, Elsevier - Academic Press, 2005.

[30] LJ. Stanković, "A measure of some time-frequency distributions concentration", *Sig. Proc.*, Vol. 81, No. 3, Mar. 2001, pp. 621-631.

[31] K. M. Aamir, M. A. Maud, A. Loan, "On Cooley-Tukey FFT method for zero padded signals," in *Proc. of IEEE Int. Conf. on Emerg. Techn.*, Sept. 2005, pp. 41-45.

[32] C.-M. Kao, X. Pan, M. A. Anastasio, and P. L. Rivera, "An interpolation method using signal recovery and discrete Fourier transform," in *Proc. of IEEE Nucl. Science Symp.*, Vol. 2, 1998, pp. 1387-1391.

[33] V. Popović, M. Daković, T. Thayaparan, and LJ. Stanković, "SAR images improvement by using the S-method," in *Proc. of ICASSP'06*, Toulouse, France, 2006.

[34] D. S. Pham and A. Zoubir, "Analysis of multicomponent polynomial phase signals", *IEEE Trans. Sig. Proc.*, Vol. 55, No. 1, Jan. 2007, pp.56-65.

[35] A. D. Lazarov, and Ch. N. Minchev, "SAR imaging of a moving target," in Proc. of RAST 2007, Istanbul, Turkey, June 2007, pp. 14-16.